COBEM 2023 27TH INTERNATIONAL CONGRESS OF MECHANICAL ENGENEERING

ABCM Brazilian Society of Mechanical Sciences and Engineering
27th ABCM International Congress of Mechanical Engineering
December 04-08, 2023, Florianópolis-SC, Brazil

COBEM-2023-0497
DIRECT NUMERICAL SIMULATION OF TURBULENT FLOW OF POWER-LAW FLUIDS IN AN ANNULAR PIPE

L. L. Palladino
Graduate Program in Mechanical Engineering (PGMec), Federal University of Paraná (UFPR). Curitiba, Paraná, Brazil.

D. B. Pitz
Graduate Program in Mechanical Engineering (PGMec). Department of Mechanical Engineering, Federal University of Paraná (UFPR). Curitiba, Paraná, Brazil.

Abstract. *Non-Newtonian fluids are present in a wide range of applications within industrial processes, such as polymer processing and many biological flows. The understanding of turbulent flows of non-Newtonian fluids remains substantially unsolved, since their behavior gets increasingly complex compared to Newtonian fluids, which already have their own complexity when it comes to turbulence. Flows encountered both in nature and in engineering are usually turbulent due to the high velocities and resulting shear stresses involved. For this reason, canonical problems are used to investigate fundamental aspects of a certain problem and to verify the accuracy of the solutions found, such as flows in channels and pipes. Fully developed turbulent concentric annular pipe flow is an interesting subject with important applications in engineering. One motivation for studying annular flows of GNFs (Generalized Newtonian Fluids) comes from the Oil and Gas sector, particularly in the application of perforation mud during oil well drilling. The flow physics in a concentric annular pipe flow is more complex than in a circular pipe flow since it has two walls with different curvatures instead of one. In this work, a Spectral Element-Fourier Method (SEM) for Direct Numerical Simulation (DNS) of the Navier–Stokes equations is used to evaluate turbulent statistics of flow of a non-Newtonian fluid through a pipe with an annular cross section. A power-law rheology model is used for the GNF. Average velocity profiles and Reynolds stresses obtained from the DNS are compared to an annular concentric Newtonian fluid turbulent flow. It is expected that this investigation sheds light on how the flow index n of the power-law model influences the flow statistics.*

Keywords: *DNS, GNF, Turbulent flow, Annular pipe, Power-law fluids*

1. INTRODUCTION

One of the main interests of the study of flows in annular pipelines comes from the Oil and Gas industry, especially for applications in drilling in oil wells. Drilling fluids are usually colloidal suspensions based on water or oil. Additives are usually mixed with the fluid to modify its drilling properties, such as barite to increase mud density, polymers to modify filtration rates or to act as viscosifiers, which can influence the rheology of the fluid significantly (Escudier and Gouldson (1995)).

In drilling operations, a flow in annular geometry cannot be conducted with very slow velocities (laminar regime) to avoid sedimentation of the gravel to the bottom of the well and cannot be extremely turbulent as this impairs the stability of the well. Therefore, it is very important to better understand the phenomenon of turbulent flow in tubes with annular sections (Epelle and Gerogiorgis (2017)).

The application of this Direct Numerical Simulation (DNS) technique to non-Newtonian fluid flows allows the rheological model to be treated in more detail and has the potential to allow the effect of different rheological parameters to be correctly quantified and understood. Furthermore, DNSs can provide benchmark results for testing and validating turbulence models, which is quite interesting for studies involving non-Newtonian fluids, an area where turbulence modelling is still incipient.

A key problem in obtaining accurate results for turbulent flow of real non-Newtonian fluids using DNS is the difficulty of approximating real rheology over a very wide range of shear rates using any of the simple generalized Newtonian rheological models. In practice, it is possible to approximate the fluid behaviour for a certain range of shear rates, however it is quite difficult to exactly reproduce the real fluid behaviour in computer simulations (Mezger (2006)).

Over the years, extensive research has been devoted to the study of fluid flows in pipes, encompassing both non-Newtonian fluids and Newtonian fluids. Chung *et al.* (2002) conducted a study focused on using DNSs to investigate the Newtonian fluid turbulent flow in concentric annular pipes, aiming to enhance the understanding of this complex fluid dynamics scenario. This involves investigating the velocity profiles, flow structures, and turbulence characteristics within the concentric annular pipe configuration. Annular pipes, consisting of an inner and outer pipe, possess distinct flow

characteristics and exhibit phenomena that differ from those observed in single-pipe flows. Bagheri *et al.* (2020) perform DNS of Newtonian fluid flows in annular pipes for investigating the influence of domain size on various flow parameters, including velocity profiles, turbulent statistics, and flow structures.

Simultaneously, investigations into non-Newtonian fluid flows in pipes, have also been the subject of substantial scientific inquiry. Studies performed by Rudman *et al.* (2004) shows how the rheological models influences the flow statistics of a non-Newtonian fluid flow in pipes. Singh *et al.* (2017) conducted a study that investigates the impact of shear thinning on the flow statistics of turbulent pipe flow of power-law fluids through DNSs. It briefly explores an alternative scaling that allows the recovery of the law of the wall. With shear-thinning, the mean viscosity slightly increases at the wall, and its profile appears to exhibit a logarithmic relationship in the velocity log layer.

While studies on non-Newtonian fluid flows in pipes and Newtonian fluid flows in annular pipes have been conducted individually, there remains a gap in the existing literature that comprehensively explores the interplay between these two areas. Investigating the behavior of non-Newtonian fluids in annular pipe geometries is crucial for addressing practical scenarios where complex fluids encounter varying flow conditions. By addressing the gap in knowledge concerning non-Newtonian fluid flows in annular pipes, this study aims to contribute to the development of efficient and accurate models for predicting fluid behavior in various industrial applications though the evaluation of the flow statistics for different rheological parameters.

2. METHODOLOGY

The methodology employed in this study involves conducting DNSs to investigate the flow behaviour of a non-Newtonian fluid with a power-law rheology model for different power-law indices n in a concentric annular pipe geometry. In general, DNSs provide detailed information of the velocity field and its evolution over time for simple geometries and relatively small Reynolds numbers. Furthermore, there is no need for turbulence models to parameterize the influence of turbulent vortices, since each of these vortices, from the largest to the smallest, is computed. Starting from the specified initial conditions, the Navier-Stokes equations are integrated in time over some specified domain. DNSs are comparable to experimental realizations only on the computer, and not in a wind tunnel, for example (Davidson (2015)).

By utilizing the DNS approach with a power-law rheology model and the SEM, this methodology offers a comprehensive framework for investigating the flow characteristics of non-Newtonian fluids within annular pipe geometries. It facilitates the accurate representation of the complex fluid behaviour, providing valuable insights into the flow dynamics, velocity profiles, and turbulence characteristics within the system.

The current study considered a concentric annular tube geometry with a radius ratio equivalent to 0.5 as shown in Figure 1. The values for the Reynolds numbers based on the friction velocities were extracted from the study of Chung *et al.* (2002), in order to validate the results for the analysis with the fluid with a power-law index $n = 1$ (Newtonian fluid).

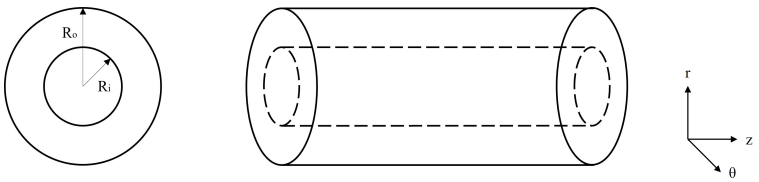

Figure 1. Concentric annular pipe geometry

The Reynolds number based on the friction velocity Re_τ is of crucial importance in DNSs, particularly for turbulent flows. The significance of this number lies in its role in determining the flow regime and characterizing the behavior of turbulent structures. It is calculated by dividing the product of the shear wall velocity u_τ and a characteristic length scale δ by the kinematic viscosity of the fluid ν. Mathematically, it can be expressed as:

$$Re_\tau = \frac{u_\tau \delta}{\nu}, \tag{1}$$

For a concentric annular pipe, the characteristic length scale δ is defined as the half of the distance between the inner and the outer walls, as expressed by Eq. 2:

$$\delta = \frac{R_o - R_i}{2} \tag{2}$$

2.1 RHEOLOGICAL MODEL

Non-Newtonian fluids are classified as those that present variable viscous behaviour for different conditions. In general, they are fluids that do not obey Newton's law of viscosity, i.e., the shear stress is not simply directly proportional to

the shear rate through a constant. There is a wide range of models that seek to describe non-Newtonian fluids, such as pseudoplastic, viscoplastic, viscoelastic and thixotropic fluids.

Due to this behavior of viscosity, the relationship between shear rate and shear stress of fluids are different. In the Newtonian fluid this relationship is linear and in non-Newtonian fluids, besides not being linear, it can still be dependent on time. Some examples of non-Newtonian fluids are paints, polymers, molten plastics, toothpaste, gasoline, synovial fluid found in joints, blood and other organic fluids (Yamaguchi (2008)).

Most polymers exhibit shear-thinning, temperature, and pressure dependent viscosities. The shear-thinning effect is defined as the reduction of viscosity at high strain rates. This phenomenon is explained by the fact that molecular chains are disentangled and stretched at high strain rates, which makes them able to slide over each other more easily, which in turn decreases the polymer viscosity. To take these non-Newtonian effects of viscosity dependence into consideration, neglecting viscoelastic effects, it is common to define the viscosity as a function of strain rate and temperature. To this end, some rheological models have been developed over the last decades to define an accurate criterion to describe the viscous behaviour of a Generalized Newtonian Fluid (GNF), i.e. fluids whose viscosity depend on the shear rate while more complex effects such as viscoelasticity are neglected (Mezger (2006)).

There are a variety of substances for which the mechanical properties differ from Newton's law of viscosity to a greater or lesser degree. The rheological characterization of GNFs is made by means of experimental analysis (Yamaguchi (2008)).

The power-Law model, proposed by Ostwald and de Waele, is a simple model that accurately represents the shear region in the viscosity curve by shear stress; however, it does not consider the Newtonian plateau observed for small strain rates. The model is described by Eq. 1 (Mezger (2006)).

$$\eta = k\dot{\gamma}^{n-1}, \tag{3}$$

where k represents the consistency parameter, $\dot{\gamma}$ the shear rate magnitude and n is the power-Law index, where 1 indicates that the fluid has Newtonian behaviour, and $n < 1$ and $n > 1$ indicate, respectively, shear-thinning and shear-thickening behaviour.

2.2 SPECTRAL ELEMENT METHOD

The Spectral Elements Method (SEM) is a numerical technique that combines FEM (Finite Element Method) and spectral methods to solve partial differential equations in Computational Fluid Dynamics (CFD) and structural mechanics. SEM offers high accuracy solutions and provides several advantages. It allows flexibility in choosing interpolation functions, handles complex geometries effectively, achieves fast convergence, and exhibits lower numerical dispersion and dissipation errors. However, SEM also has limitations, including computational cost, complex implementation, challenges in mesh generation, stability issues for certain problems, and increased preprocessing and post-processing efforts. While SEM delivers high accuracy and spectral convergence, it may require more computational resources and specialized knowledge compared to simpler methods (Canuto *et al.* (2010)).

In a standard low-order FEM formulation, a given differential equation is multiplied by a weight function, the solution is locally approximated by a linear function and the resulting equation is integrated over the domain, which is divided into several non-overlapping elements. The mesh refinement then consists of decreasing the element size h. In a spectral element formulation, the functions used to approximate the solution are high-order polynomials, thus allowing the resolution to be refined by decreasing the element size h or increasing the polynomial order p (Karniadakis and Sherwin (2013)).

2.3 SEMTEX - SEM CODE

In this work, the spectral element code Semtex (Blackburn and Sherwin (2004)) was employed. In the code, a spectral element–Fourier formulation is employed, originally proposed by Karniadakis (1990). Semtex is a suite of simulation codes based on the SEM, primarily designed for DNS of incompressible flows. Semtex employs isoparametrically mapped two-dimensional quadrilateral elements, utilizing the Gauss-Lobatto-Legendre (GLL) nodal shape function basis and continuous Galerkin projection. To extend its capability to three-dimensional problems, Semtex incorporates Fourier expansions in an orthogonal direction. An important feature of Semtex is its ability to handle problems in both Cartesian and cylindrical coordinate systems (Blackburn and Sherwin (2004)).

Using Fourier expansions in one direction is an efficient way to investigate problems where one direction is homogeneous, such as channel and pipe flows, or if the geometry is axisymmetric in cylindrical coordinates, where the azimuthal direction is naturally homogeneous. The discretization of the spectral element is obtained using a nodal expansion basis. In particular, the Lagrange polynomials interpolated at the GLL nodes are considered. Only quadrilateral elements are allowed, so that the two-dimensional expansion basis is constructed from the tensor product of one-dimensional bases. Therefore, the three-dimensional expansion basis used in the Semtex code can be written as:

$$\phi_{pqr}(\xi_1, \xi_2, \xi_3) = h_p(\xi_1) h_q(\xi_2) e^{iz\beta\xi_3}, \tag{4}$$

where $\beta = \frac{2\pi}{L_{\xi 3}}$ is the wave number, and $L_{\xi 3}$ is the length of the domain along the homogeneous direction. The use of Fourier expansions in one direction allows an efficient evaluation of the derivatives in Fourier space, and the Fast Fourier Transform (FFT) algorithms are used to transfer to physical space, and vice versa. Due to the linearity of the Fourier transform operator, the complete three-dimensional problem is reduced to two-dimensional problems, one for each Fourier plane. This separation provides a natural way to parallelize computations simply and efficiently and forms the basis of the parallelization strategy used within Semtex. However, this limits the number of processors that can be used for the number of Fourier modes configured in a given numerical analysis. The time integration is based on the semi-implicit, stiffly stable velocity correction scheme proposed by Karniadakis *et al.* (1991). The incompressible Navier–Stokes equations are employed with a spatially variable viscosity η as (Rudman *et al.* (2004)):

$$\partial_t \vec{u} + \vec{N}(\vec{u}) = -\frac{1}{\varrho}\nabla p + \frac{1}{\varrho}\nabla \cdot \left[\eta \left\{\nabla \vec{u} + (\nabla \vec{u})^T\right\}\right], \tag{5}$$

$$\nabla \cdot \vec{u} = 0, \tag{6}$$

where $\vec{N}(\vec{u})$ represents the non-linear terms and is calculated according to Eq. 7:

$$\vec{N}(\vec{u}) = (1/2)(\vec{u} \cdot \nabla \vec{u} + \nabla \cdot \vec{u}u) \tag{7}$$

In order to handle the viscous terms in a semi-implicit manner, the non-Newtonian viscosity is separated into a spatially constant component η_r, and a spatially varying component $\eta - \eta_r$. This approach improves the overall numerical stability of the method (Singh *et al.* (2017)). The main idea is to ensure that the reference viscosity (η_r) is consistently greater than the local viscosity across most of the domain and most of the time (Rudman *et al.* (2004)).

To initially estimate the reference viscosity (η_r), the estimated viscosity at a shear rate equal to the superficial flow velocity divided by the pipe radius is chosen. It is crucial to avoid selecting an excessively small value of η_r, as it would result in stability problems or requiring very small time steps. On the other hand, choosing a value that is too large also leads to instability for reasons that are not fully understood (Singh *et al.* (2017)). To induce flow in the axial (z) direction, a body force per unit mass is introduced in the z-momentum equation so the pressure becomes periodic in the axial direction (Rudman *et al.* (2004)).

3. COMPUTATIONAL PARAMETERS

In this study the bulk Reynolds number based on the hydraulic diameter, $Re_{Dh} = U\, D_h/\nu$ was kept constant at 8900, and the power-law index n was varied such that $n = 0.6, 0.8, 1.0$ and 1.2 were chosen. In the simulations for $n = 0.6$ the turbulent fluctuations were suppressed to a point where the flow became laminar; therefore, the results for this case will not be presented here.

To start the simulations, small-amplitude sinusoidal perturbations were added to a laminar velocity profile, and white noise was further added to perturb all the Fourier modes. Transition was monitored through the energy of Fourier modes and the total wall shear stress. After the transition to turbulence, statistics were not collected until ten flow-through times (FTT) had passed. For each case, ten FTTs were sufficient to achieve time-converged first- and second-order statistics. The simulations were first run for $n = 1$ (Newtonian case). The cases $n = 0.8$ and $n = 1.2$ were then run using an instantaneous flow field from $n = 1.0$ as an initial condition.

The computational domain was discretized with $N_{el} = 600$ spectral elements in the $r - \theta$ plane with polynomial order $N_P = 8$, and $N_Z = 384$ planes in the axial direction. These and other parameters used in the simulations are shown in Table 1. Note that the radius ratio R_i/R_o was kept fixed at 0.5 for all simulations.

Table 1. DNS Parameters

R_i/R_o	N_P	N_z	$Re_{\tau i}$	$Re_{\tau o}$	$\Delta^+_{r,min}$	$\Delta_{r_i}\theta^+$	$\Delta^+_{r_o\theta}$	Δz^+
0.5	8	384	153	144	0.6	3.9	7.8	9.8

The resolutions achieved in the simulations are consistent with those used, for instance, by Chung *et al.* (2002) and Bagheri *et al.* (2020). Note that the values of $Re_{\tau,i}$ and $Re_{\tau,o}$ differ slightly due to the different curvatures and resulting different shear stresses of the inner and outer walls of the annular pipe.

4. RESULTS AND DISCUSSION

4.1 Mean Fourier Modes Energy

Figure 1 shows the temporal average values of energies in the various Fourier modes and it indicates that the resolution is suitable due to a separation of about four and a half decades between the highest and smallest wave numbers, which

indicates that the DNS is well resolved since the small turbulent scales were achieved. The GNF with n=1.2 exhibits shear-thickening behaviour, while the GNF with n=0.8 shows a shear-thinning behaviour. This means that as the stress or shear rate increases, the viscosity decreases. This unique property is characteristic of many non-Newtonian fluids. The curve for the GNF with n=0.8 lies bellow the Newtonian fluid as expected, since this fluid flow has more tendency to become laminar, as the higher modes have less energy compared to n=1.2.

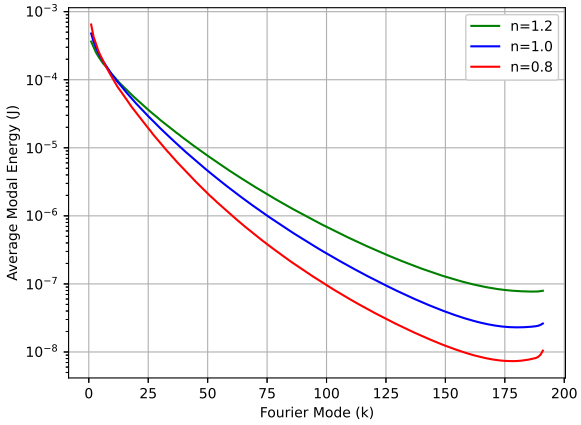

Figure 2. Mean modal kinetic energy as a function of the axial Fourier mode k for different flow indices n.

4.2 Mean Flow Properties

Figure 3 shows the mean velocity profile for the annular pipe flow for each power-law index n for both inner and outer walls considering a radial dimensionless distance from the inner wall parameter $r^+ = u_{\tau_i}(r - R_i)/\nu$ and from the outer wall $r^+ = u_{\tau_o}(R_o - r)/\nu$. The dashed lines represent the linear and the logarithmic part of the law of the wall for a Newtonian fluid. The velocity profiles shown in Fig. 3 indicate that the higher the power-law index n is, the more displaced down the law of the wall the curve of this fluid will be. This is quite reasonable, as a fluid with a higher n-index will consequently have a higher viscosity, which entails a higher friction force in the wall regions. Figure 3 indicates that the outer wall of the annular pipe apparently has slightly larger influence on activating turbulent structures, as also observed by Chung *et al.* (2002) and by Bagheri *et al.* (2020).

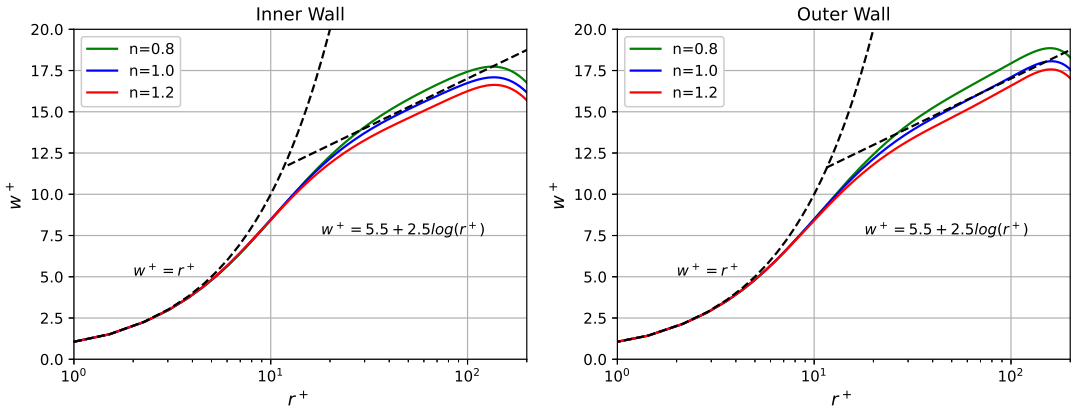

Figure 3. Mean velocity profiles in wall units near the inner and outer walls. The dashed lines represent profiles for the viscous sub-layer and log law of the wall for n = 1.0.

4.3 Velocity Fluctuations

Figure 4 and Figure 5 show rms distributions for velocity fluctuations values in friction velocity units for axial (z) and radial (r) directions respectively. When comparing the inner and outer walls, it is evident that the turbulent intensities of the inner wall are lower than those of the outer wall. This disparity in turbulent kinetic energy can be attributed to the transverse curvature effect (Chung *et al.* (2002)). The inner wall, having a smaller surface area compared to the outer

wall, supplies a relatively smaller amount of turbulent kinetic energy. Turbulence production follows similar trends to pipe flow of power-law fluids as shown in Singh *et al.* (2017).

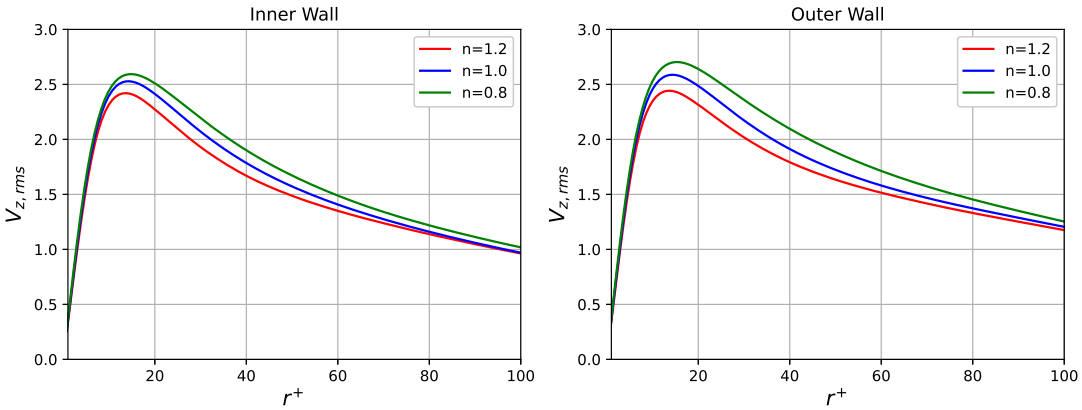

Figure 4. RMS axial (Z) velocity fluctuations normalised by the wall shear velocity

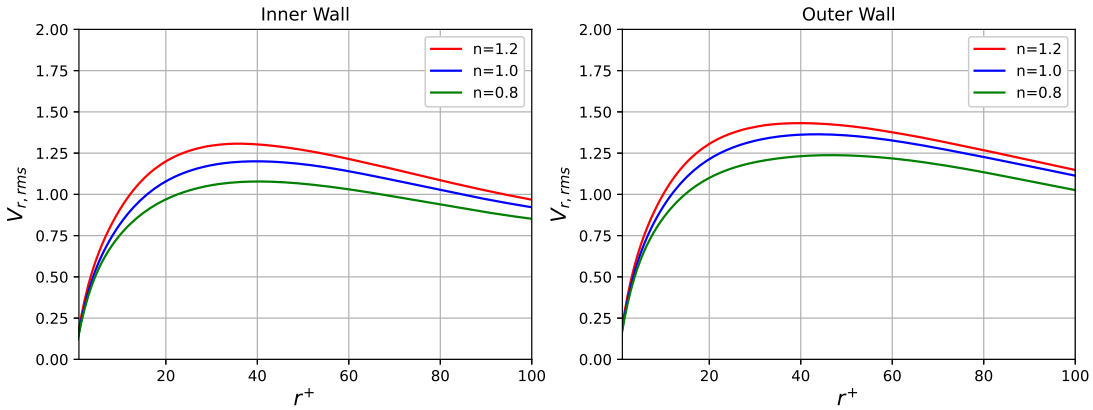

Figure 5. RMS radial (R) velocity fluctuations normalised by the wall shear velocity

4.4 Reynolds Stresses

Figure 6 shows Reynolds stresses non-dimensionalized by the mean wall friction velocity. Reynolds stresses follow similar behaviour of power-law fluids as showed in Singh *et al.* (2017). It is interesting to note that the Reynolds stress is higher near the outer wall compared to the inner wall, as well as the RMS velocity distributions.

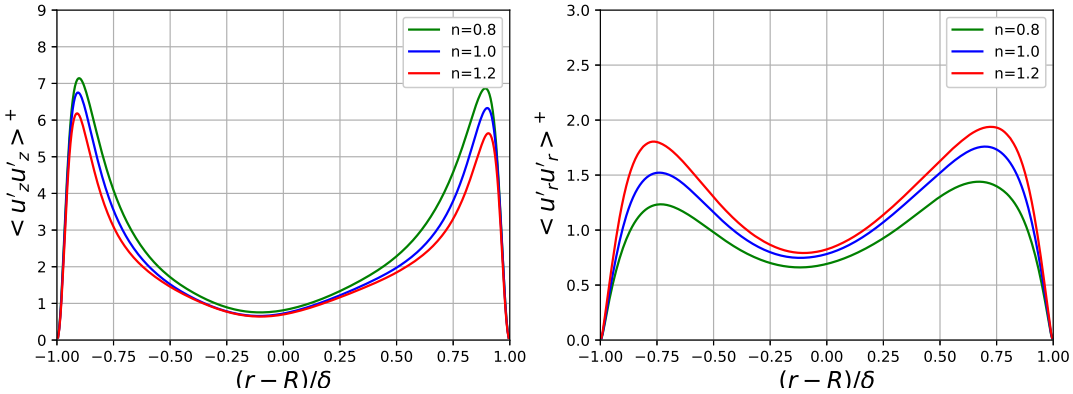

Figure 6. Distribution of Reynolds axial (z) and radial (r) stress

4.5 Instantaneous Velocity Contours

Figure 7 shows a cross-section along axial (z) direction of the annular pipe with the instantaneous axial velocity. Note that the stronger the shear-thickening behaviour the fluid is, the stronger the turbulent vortices generated on both inner and outer walls are. The results are consistent with the behaviour observed by Singh *et al.* (2017), which indicate that the lower the power-law index gets, the more susceptible the flow tends to become laminar. This was also noted by analysing results from DNS with $n = 0.6$. As observed in Fig. 7, the instantaneous velocity contour for $n = 0.6$ shows that the flow is more likely to evolve to a laminar regime. For this reason, the turbulent statistics were not analyzed for this fluid flow.

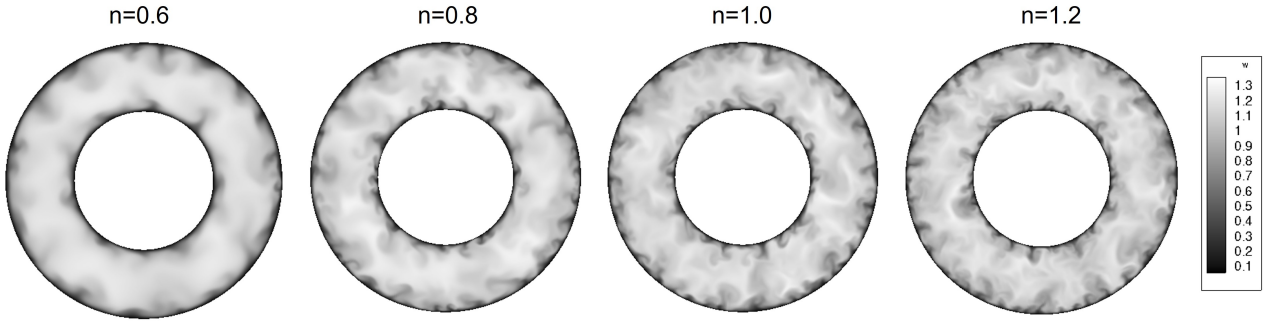

Figure 7. Instantaneous velocity contours for different power-law indices n.

5. CONCLUSIONS

A numerical study was conducted to examine the influence of power-law indices n for GNFs and of transverse curvature on near-wall turbulent structures in turbulent concentric annular pipe flow. Statistical descriptions of turbulent quantities were obtained through DNSs of turbulent concentric annular pipe flow at a Reynolds number based on hydraulic diameter, considering a radius ratio of 0.5. The mean velocity distribution showed good agreement with prior studies for annular pipe with Newtonian fluids conducted by Chung *et al.* (2002) and by Bagheri *et al.* (2020) and for GNF flow in a pipe conducted by Singh *et al.* (2017) and Rudman *et al.* (2004). Notably, it was observed that the inner profile exhibited a lower slope than the outer profile in the logarithmic region. The findings for all the non-Newtonian fluids were consistent with those reported by Rudman *et al.* (2004) for turbulent pipe flow of power-law fluids, indicating the presence of larger, weaker turbulent structures for non-Newtonian fluids compared to Newtonian fluids, along with smaller friction factors at a fixed Reynolds number.

As more shear-thinning behaviour the GNF has, the more likely to become laminar the flow is. Furthermore, as the yield stress increased, the mean flow profile deviated more significantly from both the Newtonian and power-law profiles. The turbulent structures in proximity to the outer wall exhibit greater turbulence activation when compared to those near the inner wall, as also observed in Chung *et al.* (2002) and in Bagheri *et al.* (2020).

6. ACKNOWLEDGEMENTS

The authors acknowledge the FINEP agency (projects CT-INFRA/UFPR) and Laboratório Nacional de Computação Científica (LNCC; project SIMTurb) for providing the computational resources used in this investigation. L.L.P. acknowledges the CAPES foundation for providing a scholarship.

7. REFERENCES

Bagheri, E., Wang, B.C. and Yang, Z., 2020. "Direct numerical simulation of the turbulent flow in a pipe with annular cross section". *Physics of Fluids*, Vol. 32, p. 065105.

Blackburn, H.M. and Sherwin, H.M., 2004. "Formulation of a galerkin spectral element-fourier method for three-dimensional incompressible flows in cylindrical geometries". *Journal of Computational Physics*, Vol. 197, pp. 759–778.

Canuto, C.G., Hussaini, Y.M., Quarteroni, A. and Zang, A.T., 2010. *Spectral Methods: Fundamentals in single domains*. Springer.

Chung, S.Y., Rhee, G.H. and Sung, H.J., 2002. "Direct numerical simulation of turbulent concentric annular pipe flow part 1: Flow field". *Journal Of Heat and Fluid Flow*, Vol. 23, pp. 414–443.

Davidson, P.A., 2015. *Turbulence: An Introduction for Scientists and Engineers*. Oxford University Press, Oxford.

Epelle, E.I. and Gerogiorgis, I.D., 2017. "A multiparametric cfd analysis of multiphase annular flows for oil and gas drilling applications". *Computers Chemical Engineering*, Vol. 106, pp. 645–661.

Escudier, M.P. and Gouldson, I.W., 1995. "Concentric annular flow with centerbody rotation of a newtonian and a shear-thinning liquid". *International Journal Of Heat And Fluid Flow*, Vol. 16, pp. 156–162.

Karniadakis, G.E., 1990. "Spectral element-fourier methods for incompressible turbulent flows". *Computer Methods in Applied Mechanics and Engineering*, Vol. 80, pp. 367–380.

Karniadakis, G.E., Israeli, M. and Orszag, S., 1991. "High-order splitting methods for the incompressible navier-stokes equations". *Journal of Computational Physics*, Vol. 97, pp. 414–443.

Karniadakis, G.E. and Sherwin, S., 2013. *Spectral/hp element methods for computational fluid dynamics*. Oxford University Press, Oxford.

Mezger, T.G., 2006. *The Rheology Handbook*. Vincentz Network, Hannover.

Rudman, M., Blackburn, H.M., Graham, L.J.W. and Pullum, L., 2004. "Turbulent pipe flow of shear-thinning fluids". *Journal of Non-Newtonian Fluid Mechanics*, Vol. 118, pp. 33–48.

Singh, J., Rudman, M. and Blackburn, H.M., 2017. "The influence of shear-dependent rheology on turbulent pipe flow". *Journal of Fluid Mechanics*, Vol. 822, pp. 848–879.

Yamaguchi, H., 2008. *Engineering Fluid Mechanics*. Springer, Kyoto.

8. RESPONSIBILITY NOTICE

The authors are solely responsible for the printed material included in this paper.